

## Electrical conduction and current noise mechanism in discontinuous metal films. II. Experimental

M. Celasco,\* A. Masoero, P. Mazzetti,<sup>†</sup> and A. Stepanescu

*Istituto Elettrotecnico Nazionale Galileo Ferraris-Torino, Italy  
and Gruppo Nazionale di Struttura della Materia del Consiglio Nazionale delle Ricerche,  
U.R. 24-Corso Massimo d'Azeglio, 42-Torino, Italy*

(Received 13 July 1977)

Experimental results concerning the electrical conductance, the conductance noise, and the effects of ion migration and diffusion on discontinuous gold films, in a wide range of temperatures, are reported. These results are compared with the theoretical ones obtained by a theory developed in the preceding paper. It is shown that this theory well explains the conductance behavior of the films in a wider temperature range than previous theories and gives the right shape and the correct magnitude for the conductance noise power spectrum. A discussion about some discrepancies between theory and experiments, probably due to the fact that the actual structure of the film has not been properly taken into account, is also given in the text.

### I. INTRODUCTION

In the preceding paper (known hereafter as I) a theoretical model of electrical conduction and noise formation in ultrathin metal films (30–100 Å thick) was developed. The aim of this paper is to present a picture of the experimental situation showing that most of the results can be well accounted for by the theory.

The reported experimental results were obtained in our laboratory and cover a temperature range larger than in the current literature. They concern discontinuous gold films evaporated in ultrahigh vacuum on different types of substrates (sapphire, fused silica, quartz, mica) and deal with several properties as electrical conductivity versus temperature, current noise related to conductivity fluctuations in different physical conditions, and field effect due to ion migration in the substrate. It will be shown that the theory proposed in I well explains the behavior of the conductivity versus temperature in an extended range of temperatures for films having different thicknesses. It should be noted that for all the films the Arrhenius plot for the conductivity is far from being a straight line, as generally assumed by many authors, who try to fit the data with an activated type of conduction process. Actually, that fit can be done in a rather restricted temperature range.<sup>1-10</sup> For what concerns the noise, the theory gives the correct order of magnitude for its intensity as well as the correct shape of the power spectrum. Theories on the conductivity in discontinuous films, based on simple tunneling, or trap-assisted tunneling or hopping, without assuming the modulation effect on the potential barrier due to the fluctuating surface charge described by Eq. (7-1)<sup>11</sup> would yield a noise many orders of magni-

tude smaller. Owing to the simplifying assumptions made, the theoretical expressions do not reproduce all the experimentally observed features of the spectra as, for instance, the change in the slope of the power spectrum consistently observed at the highest temperatures. These discrepancies are, however, qualitatively well understood and discussed in Sec. V, where the main lines of an improved theory are also shown.

### II. ELECTRICAL CONDUCTIVITY

#### A. Experimental techniques

The experimental results reported here refer to discontinuous gold films obtained by electron-beam evaporation of gold in ultrahigh vacuum ( $10^{-9}$  mbar). Different types of insulating substrates were used: sapphire, fused silica, quartz, and mica. The typical structure of the films, after annealing at 500 °C, is represented in Figs. 1(a) and 1(b). It is characterized by large islands separated by gaps which are also generally large, but become very small in critical points where electrical conduction from one island to another takes place. As shown in the following, the smallest distance of the islands must be of the order of few tens of Angstroms, to account for observed conductivity of these films by tunneling. The evaporation rate and electrical conductance of the films have been controlled during the deposition on the substrate, which was kept at about 250 °C to ensure a good adherence of the gold on the substrate. All the results were obtained directly on the films within the vacuum system after annealing at 500 °C for several hours to avoid structural changes on the subsequent measurements. All the reported experimental results refer to films having the following dimensions: length = 2.5 mm,

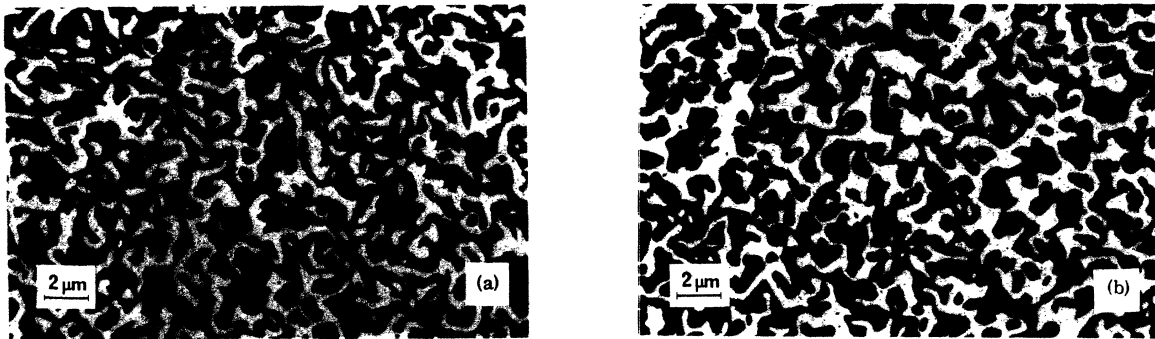


FIG. 1. Electron micrograph of discontinuous Au film structure on fused silica substrate after annealing at 500 °C in vacuum ( $10^{-9}$  mbar): (a) film with islands metallically connected and very low surface resistance ( $1.5 \Omega/\square$ ); (b) film with islands separated by very large gaps and practically infinite surface resistance.

width = 1.5 mm. Average thickness of the films was between 30 and 100 Å.

B. Conductivity versus temperature

Typical results on the electrical conductivity versus temperature of gold films deposited on dif-

ferent types of substrates are reported in Fig. 2. They are representative of a long series of measurements, all showing the same behavior. The temperature range was in most cases from liquid-nitrogen temperature up to 725 °K. In the case of sapphire one series of measurements was extended

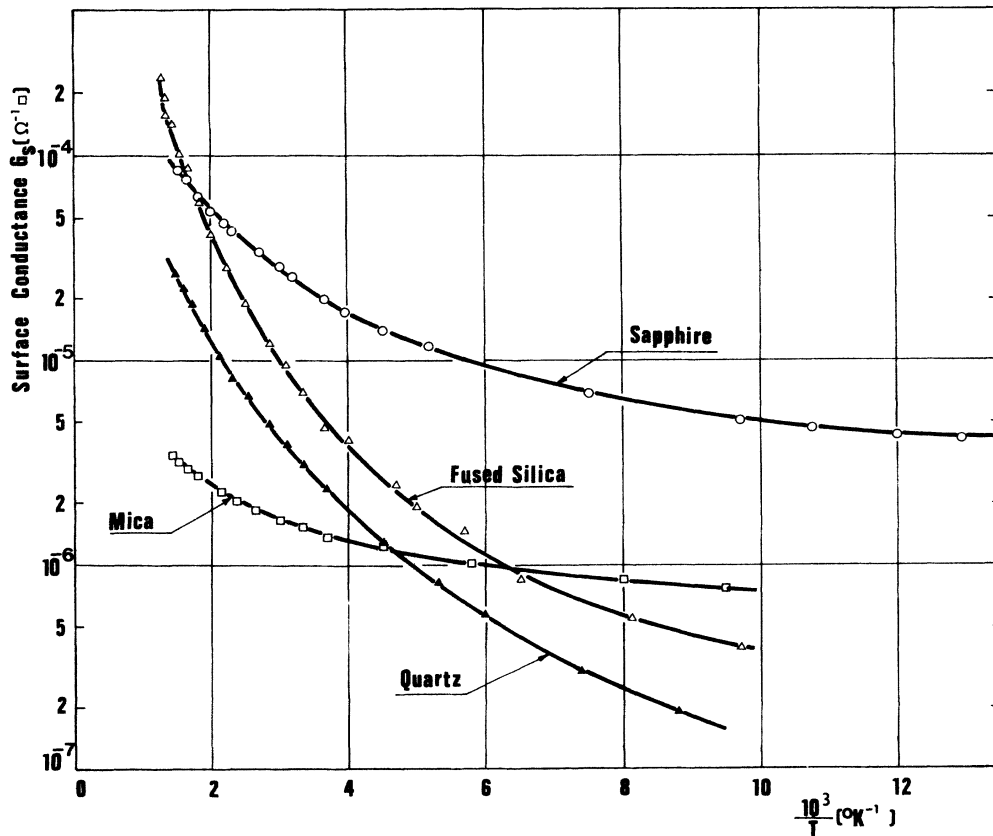


FIG. 2. Logarithmic plot of surface conductance  $G_s$  vs reciprocal temperature for discontinuous Au films evaporated on different substrates after annealing at 500 °C in vacuum ( $10^{-9}$  mbar). As in all the following figures, film dimensions are  $L 1.5 \times 10^{-3}$  m,  $L' = 2.5 \times 10^{-3}$  m.

down to liquid-helium temperature.

It is worth pointing out that in the whole range of temperature covered by the experiments, the behavior of the conductivity versus  $1/T$  plotted on logarithmic scale is far from being a straight line, as assumed by many authors<sup>1-8</sup> on the basis of a thermal-activated tunneling or a thermionic process, because their temperature intervals of measurements were too small. It is also interesting to note that films having about the same conductivity show a very different resistivity-thermal-coefficient plot (TCR) when deposited on different substrates: the data reported in Fig. 2 show that gold on fused silica has a conductivity change which is about one order of magnitude larger than gold on sapphire for the same temperature interval of 600°K. This is attributed mainly to the different structure of the film.

Another important point, which will be clearly interpreted by the proposed theory, is the reduction in the TCR which is consistently shown by films deposited on the same substrate when the gaps between gold islands are decreased by subsequent stages of gold evaporation (see Fig. 12). This effect has been reported in previous papers also.<sup>9,10</sup>

#### C. Impurity migration effect

In the case of  $\text{SiO}_2$  substrates having a back electrode, as shown in Fig. 3, an interesting effect was observed when a voltage drop of a few volts was applied between the film and the back electrode at a temperature above 300°C: reversible changes of conductivity occur as shown in Fig. 4. These changes can be frozen-in by simply cooling the substrate down to 180°C and can be interpreted in terms of impurity ion diffusion within the substrate.<sup>12</sup> Films deposited on a pure crystalline substrate, like sapphire, do not show any field effect. In Sec. IV these experimental results will be qualitatively explained in terms of the proposed theory.

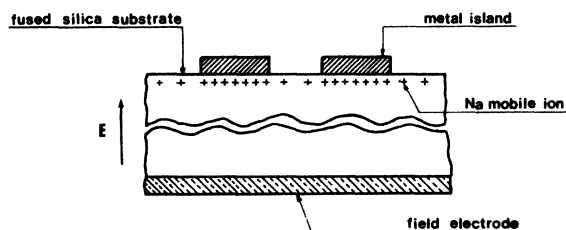


FIG. 3. Schematic picture of metal island on  $\text{SiO}_2$  substrate with a back electrode for electrical field effect experiments (Na-ion impurities are indicated).

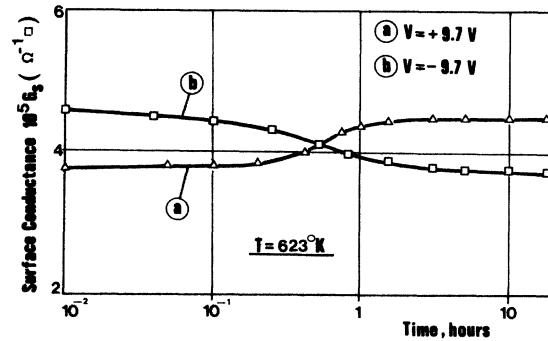


FIG. 4. Reversible change of the surface conductance  $G_s$  vs time for a discontinuous Au film at 623°K.  $V$  is the bias voltage of the film with respect to the back electrode.

#### D. Gas absorption

Experiments made on discontinuous gold films evaporated onto sapphire and silica substrates exposed to an oxygen atmosphere show that a marked reversible change of conductivity occurs upon gas diffusion within the substrate. Typical results ob-

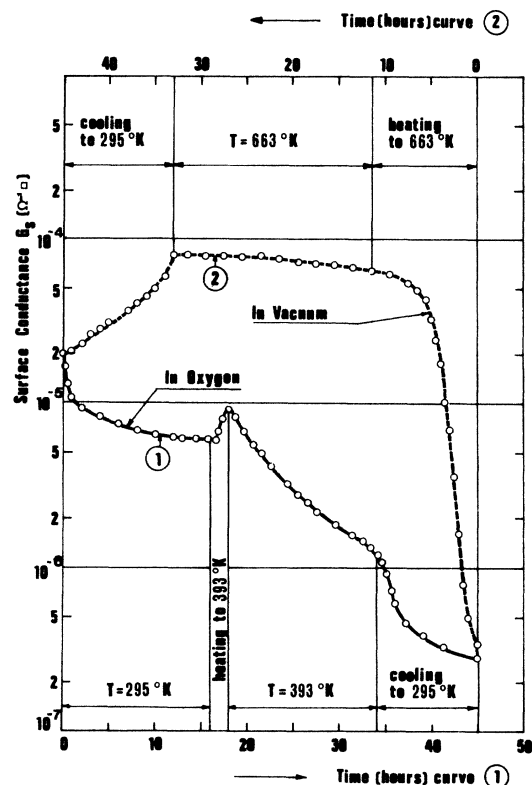


FIG. 5. Reversible changes of the surface conductance  $G_s$  vs time during exposure of the Au film to an oxygen atmosphere and after annealing in vacuum.

tained in our laboratory on gold films, having a structure as in Fig. 1, are shown in Fig. 5.<sup>13</sup>

It is seen that the conductivity variation is a rather slow process, which proves that it is associated with gas diffusion within the substrate. When the specimen is heated in vacuum, outgassing occurs and the reversible process takes place, which proves that the conductivity change is not related to structural changes of the film or to chemical reactions. As will be seen in Sec. IV this effect can be accounted for by the theory as a consequence of a reduction of the donor states density associated with oxygen diffusion.

### III. CURRENT NOISE

One of the most interesting features of the electrical conduction of discontinuous metal films is the existence of a current noise, due to the presence of spontaneous conductivity fluctuations. These fluctuations are directly related to the intrinsic conduction mechanism of discontinuous films, and become undetectable when a metallic film becomes continuous<sup>14</sup> except when current density is above an extremely high critical value.<sup>15</sup>

As stressed in I, the study of the current noise thus gives complementary information on the con-

duction mechanism of discontinuous films and can give support or rule out a given proposed model. Conductivity measurements were associated with current-noise detection and analysis. The results reported below thus refer to the same films described above. The noise measurements were made by detecting the corresponding voltage fluctuation when a constant current flows through the film. A conductivity noise,  $\langle \Delta G^2 \rangle$ , can be conveniently defined from the voltage noise  $\langle \Delta V^2 \rangle$ , as follows:

$$\langle \Delta G^2 \rangle = \langle G \rangle^2 \langle \Delta V^2 \rangle / \langle V \rangle^2, \quad (1)$$

$$\Delta G = G - \langle G \rangle, \quad (2)$$

$$\Delta V = V - \langle V \rangle, \quad (3)$$

where  $\langle G \rangle$  and  $\langle V \rangle$  are, respectively, the average of the conductivity and of the voltage across the film.

In the following, we shall report the results on current noise in terms of the dimensionless quantity  $\langle \Delta G^2 \rangle / \langle G \rangle^2$ , which is independent of the current intensity flowing in the film, owing to the fact that the voltage noise is proportional to the square of the current.

Besides the total noise intensity in a given frequency bandwidth, results on the power spectrum

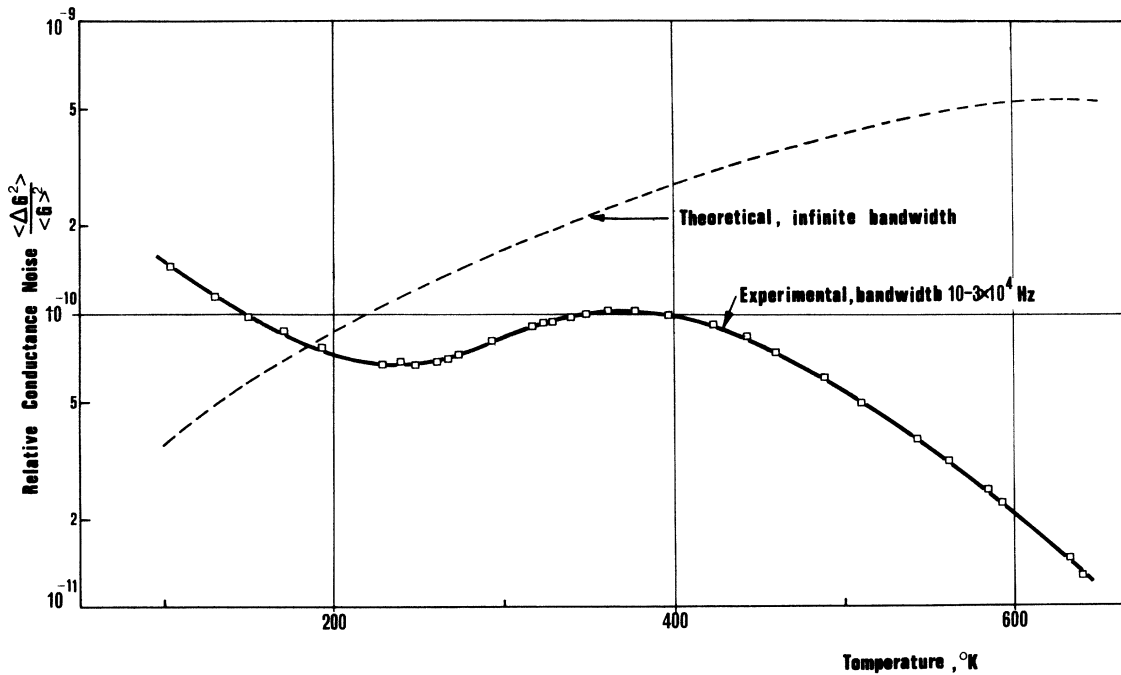


FIG. 6. Relative conductance noise  $\langle \Delta G^2 \rangle / \langle G \rangle^2$  vs temperature in a frequency band  $10-3 \times 10^4$  Hz of Au film evaporated onto sapphire substrate after annealing at  $500^\circ\text{C}$  in vacuum ( $10^{-9}$  mbar). The points are experimental, the broken line is computed from Eq. (9) with  $D=l=3 \times 10^{-7}$  m,  $\varphi_B(T)$  has been obtained by Eq. (7) with  $\delta=10^{19}$  states/m<sup>2</sup>,  $\varphi_1=0.2$  eV, and  $d=1.6 \times 10^{-9}$  m (see also Figs. 3 and 4 of paper I).

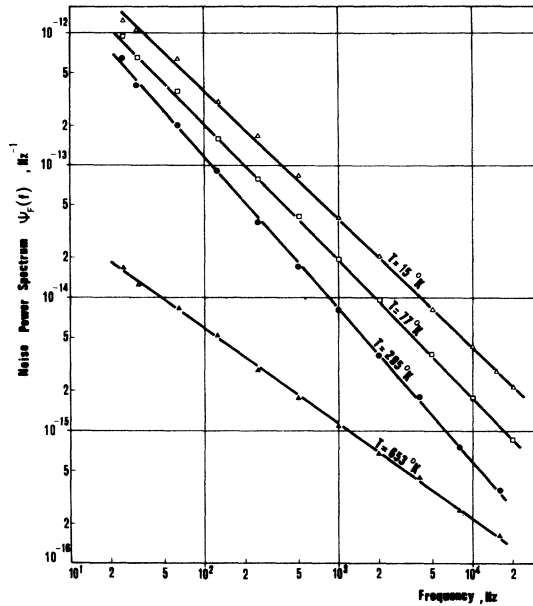


FIG. 7. Experimental power spectra of relative conductance noise  $\psi_F(f)$  at different temperatures in Au film evaporated onto sapphire substrate.

of the noise and its behavior with temperature will be reported. Noise spectra have been detected by using conventional techniques. In particular most of the results have been obtained with a model No. 3721A Hewlett Packard correlator equipped with a model No. 3720A Hewlett Packard spectrum display.

A. Current noise versus temperature

The general behavior of the integral noise in a fixed bandwidth ( $10-3 \times 10^4$  Hz) versus temperature is represented in Fig. 6, in the case of sapphire substrate. A similar behavior is shown by films deposited on other substrates, such as fused silica and mica. A well-reproducible feature is the maximum of the noise near  $400^\circ\text{K}$ , which corresponds to a change in the slope of the power spectrum as shown in Fig. 7, where the power spectrum of the noise at a temperature of  $653^\circ\text{K}$  is reported. From the same figure it is seen that over a rather large range of temperature the noise spectra are nearly of the  $1/f$  type. Also, the change in the spectrum slope, above  $500^\circ\text{K}$ , is a well-reproducible characteristic, observed without exception in all the in-

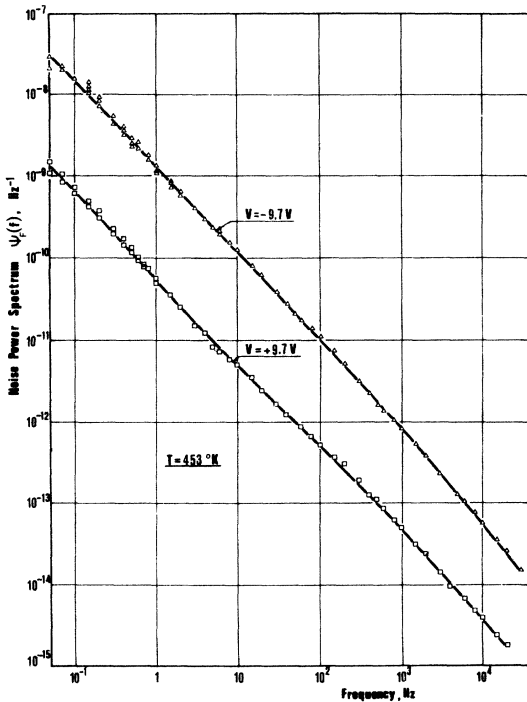


FIG. 8. Relative conductance noise power spectrum  $\psi_F(f)$  of Au film on  $\text{SiO}_2$  substrate after annealing at  $623^\circ\text{K}$  under a bias field.  $V$  is the potential of the film with respect to the back electrode (see Fig. 3).

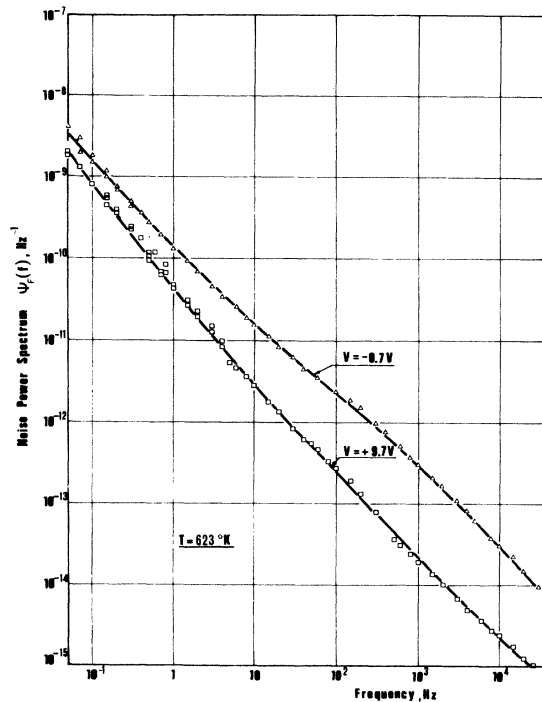


FIG. 9. Reversible change of the relative conductance noise power spectrum  $\psi_F(f)$  of Au film on  $\text{SiO}_2$  substrate after inversion of the opposite bias field at  $623^\circ\text{K}$ .  $V$  is the potential of the film with respect to the back electrode (see Fig. 3).

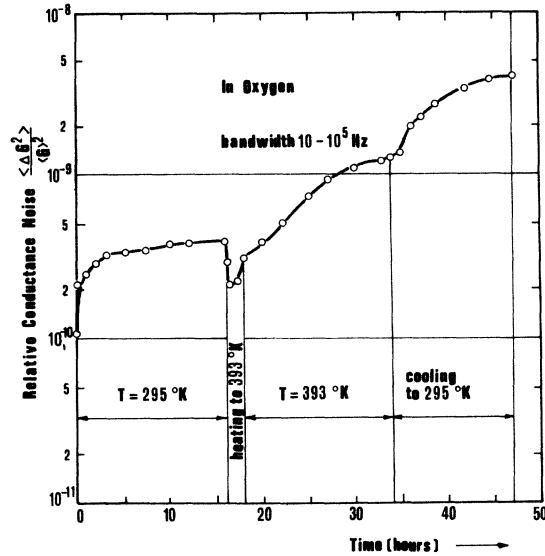


FIG. 10. Relative conductance noise  $\langle \Delta G^2 \rangle / \langle G \rangle^2$  vs time of Au film on sapphire substrate during the exposure to an oxygen atmosphere and annealed at  $393^\circ\text{K}$ .

vestigated films. Both the  $1/f$  behavior and the slope reduction of the spectrum can be explained in terms of the proposed electrical conduction mechanism as shown in Sec. IV.

#### B. Effect on noise of impurity migration and of gas absorption

The effect on the conductivity due to impurity migration or gas absorption, discussed in Secs. II C and II D are associated with a corresponding change in the noise intensity, as shown in Figs. 8, 9, and 10. In both cases the noise intensity increases when the electrical conductivity decreases. The shape of the spectrum remains of the  $1/f$  type, except at the highest temperatures, as shown in Fig. 9.

### IV. DISCUSSION

As is seen from the experimental results, the conductivity of the films versus temperature cannot be described by a simple activated process, as generally assumed,<sup>1,4-6,16</sup> when a sufficiently large temperature range is explored. Our well-annealed films showed a well-reproducible and reversible behavior from liquid-helium temperatures up to more than  $700^\circ\text{K}$ . The most remarkable effect is that the negative temperature coefficient of resistance proper of these discontinuous films tends to decrease and to become positive in the highest temperature range, the resistance value still remaining well above that pertaining to a continuous film of the same average thickness.

From Eqs. (9-I) and (34-I) the surface conduc-

tance  $G_s$  of the whole film becomes

$$G_s = G_1 + G_2, \quad (4)$$

where

$$G_1 = l(2m)^{1/2} (e/h)^2 \varphi_B^{1/2}(T) \times \exp\{-[4\pi(2m)^{1/2}/h]d\varphi_B^{1/2}(T)\} \quad (5)$$

is the tunneling conductance, and

$$G_2 = dl \frac{4\pi m^* e k^2}{h^3} T^2 e^{-\varphi_B(T)/kT} \quad (6)$$

is the thermionic conductance between two metal islands. All the symbols used above are the same as defined in I. With the value of  $\varphi_B(T)$  calculated at each temperature through the equation

$$\varphi_B(T) = \chi_m - \chi_s + \frac{e^2 d}{12\epsilon_0 \epsilon_r^*} \left[ 2d \left( \frac{m^* k T}{2\pi \hbar^2} \right)^{3/2} e^{-\varphi_B(T)/kT} - \delta e^{-[\varphi_1 - \varphi_B(T)]/kT} \right] \quad (7)$$

(obtained in Sec. II A of the paper I), the experimental results as seen in Figs. 11 and 12 are rather accurately described.

The values of the parameters involved in these equations have been discussed in paper I, where in particular, the function  $\varphi_B(T)$  versus temperature is shown, for both sapphire and silica substrates. The effective mass at the bottom of the conduction band of the insulator  $m^*$  has been assumed equal to the electron mass  $m$ . The values of  $\epsilon_r$  for sapphire and silica were taken at each temperature from Von Hippel<sup>17</sup> and MIT<sup>18</sup> reports. In the same figures, the contributions to the conductivity due to the tunneling and thermionic plus tunneling currents are shown separately. Similar results have been obtained for the case of quartz and mica substrates. The fit of the experimental results seems much better without taking into account the thermionic current, which would give a very rapid increase to the conductivity at the highest temperatures, a fact which has never been observed experimentally.

Another result which points in the same direction is the following one: during gold deposition by evaporation, the resistivity of the film drops very rapidly from infinity to extremely low values (few ohms), a fact which is well understood by taking into account the dependence of tunneling from the width of the gap between metal islands. This has been experimentally observed also at the highest temperatures, contrary to what one should expect if the thermionic effect would prevail. Indeed, the dependence of this effect on the width barrier gap is rather negligible. The results reported in Fig. 12 which refer to two films having about identical

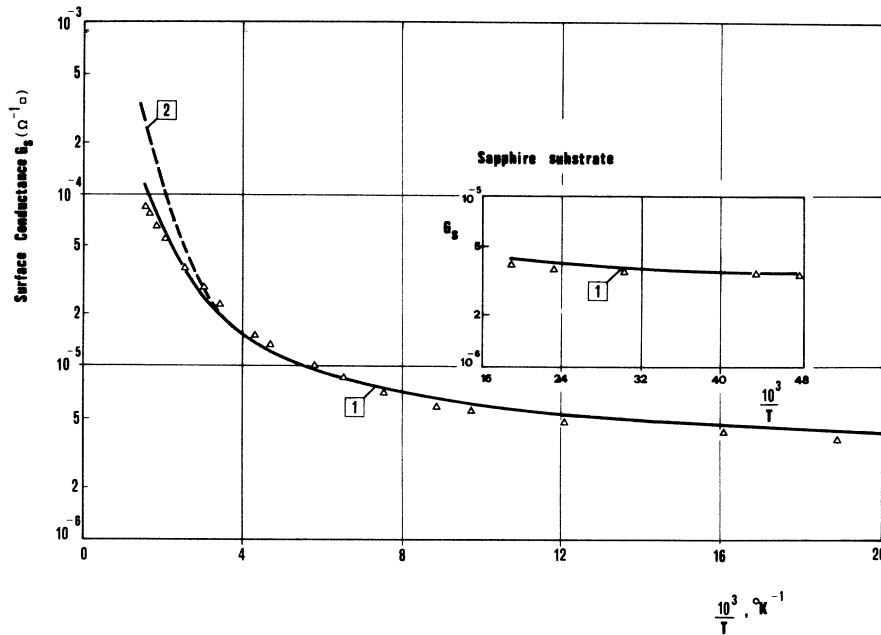


FIG. 11. Logarithmic plot of surface conductance  $G_s$  vs reciprocal temperature for an Au film evaporated onto a sapphire substrate. The points are experimental. Curve 1 is the theoretical and is computed by Eq. (5) which takes into account only the tunneling current. When the thermionic current is added (curve 2) the fitting of the experimental points becomes very bad at high temperature. The best fit parameters are:  $l = 3 \times 10^{-7}$  m;  $d = 1.6 \times 10^{-9}$  m;  $\varphi_B(T)$  is calculated from Eq. (7) with  $\delta = 10^{19}$  states/m<sup>2</sup>;  $\varphi_1 = 0.2$  eV.

structures [of the type shown in the micrographs (a) and (b) of Fig. 1] but different gap widths, match very well the conductance Eq. (4) disregarding the term  $G_2$  relative to the thermionic conductance, provided the two values of the gap width  $d$  reported in the same Fig. 12 are used. If at high temperature the thermionic current would prevail, one should expect that the conductivities of the two films would become nearly equal, as shown by broken lines. As pointed out in the Sec. IV of paper I, the fact that the thermionic current is negligible, can be explained by considering that the electron mean-free path in the conduction band of the insulator is smaller than the gap width, a fact which renders Eq. (6) invalid.

A final point about conductivity, which is well explained by the theory developed in paper I, is the fact that in general the average temperature coefficient of the resistivity is larger for films having higher electrical resistance owing to a larger average gap width between metal islands.<sup>9,10</sup> The results displayed in Fig. 12 clearly show this fact.

Concerning the current noise, the results reported in Fig. 7 clearly confirm what was anticipated in Sec. IV of paper I: the conductance noise spectra are of  $1/f$  type from helium temperature up to about 400°K. Above this temperature a reduction of the spectral density in the low-frequency range occurs and the power spectrum changes from  $1/f$  to  $1/f^\alpha$ , with  $\alpha \cong 0.7$ . A theoretical expression of the power spectrum of the relative conductance fluctuation has been obtained in paper I.

Equations (33-I) and (35-I) yield

$$\psi_F(\omega) = \frac{kT e^2 \varphi_B^{-1}(T)}{48 \pi \epsilon_0 \epsilon_r^* l} \left( \frac{4\pi(2m)^{1/2} d}{h} - \varphi_B^{-1/2}(T) \right)^2 \times \frac{1}{\omega} \left( \ln \frac{\tau'_M}{\tau'_m} \right)^{-1} [\tan^{-1}(\omega \tau'_M) - \tan^{-1}(\omega \tau'_m)] \frac{D^2 L}{L^{1/3}}, \quad (8)$$

where the meaning of the symbols is given in paper I.

Equation (8) well describes the  $1/f$  behavior of the relative conductance fluctuation spectrum of the film. In Fig. 13 the power spectrum given by Eq. (8) (multiplied by  $2 \times 2\pi$  in order to take into account that the experimental spectra refer to the frequency  $f$  and are defined only for  $f > 0$ ) is compared with the experimental spectrum relative to sapphire at room temperature. The values of the parameters involved in this equation have been taken equal to those used to fit the conductivity versus temperature curve of the film, and are reported in the figure captions. The value of  $D$  has been taken equal to  $l$ , as if the films were a structure of square islands of side  $l$ , in order to evaluate the order of magnitude of the noise intensity.

For the same purpose the logarithmic term in Eq. (8) (which represents the number of decades covered by the  $1/f$  noise along the frequency axis multiplied by 2.3) has been estimated to be of the order of 16, corresponding to seven decades. Actually, the most extended frequency range covered by experiments in which a  $1/f$  behavior of the spectrum has been found is about six decades wide (see Fig. 8). The result shows that not only the shape of the spectrum but also at least the order

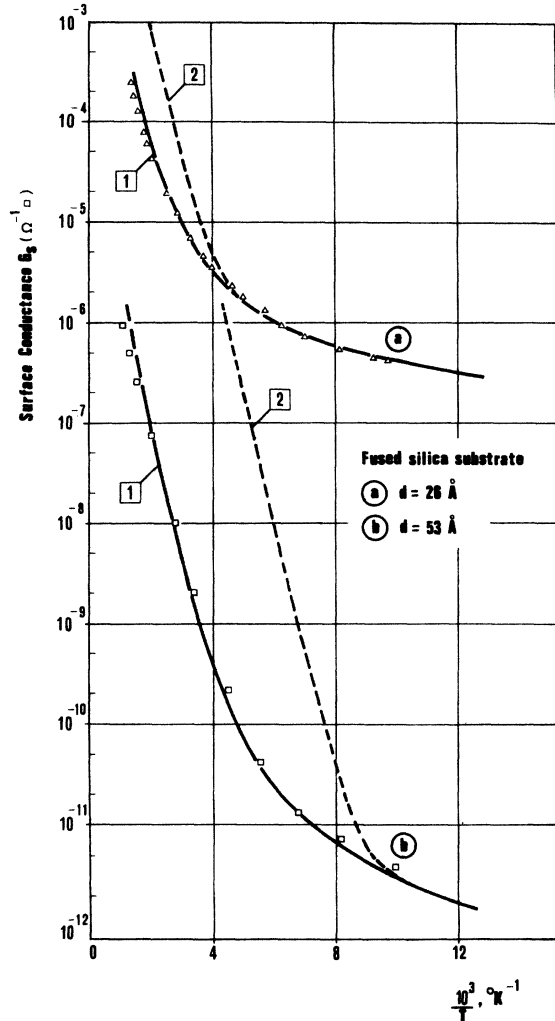


FIG. 12. Logarithmic plot of the surface conductance  $G_s$  vs reciprocal temperature for two Au films having different gap width  $d$  evaporated onto  $\text{SiO}_2$  substrates. The points are experimental. Curves 1 are theoretical and are computed by Eq. (5) which takes into account only the tunneling current. When the thermionic current is added (curves 2) the fitting of the experimental points becomes very bad at high temperatures. The best fit parameters are:  $l = 3.8 \times 10^{-6}$  m;  $\varphi_B(T)$  from Eq. (7) with  $\delta = 10^{19}$  states/m<sup>2</sup>;  $\varphi_1 = 0.25$  eV.

of magnitude of the noise intensity is correct. Previous theories,<sup>19,20</sup> which do not assume any barrier modulation effect, would give a noise estimate which is about 12 orders of magnitude lower (see Appendix). The change from the  $1/f$  behavior of the spectrum at high temperature, clearly shown in Fig. 7, is due to the change of the distribution function given by Eq. (26-I) as discussed in Sec. IIC of the paper I. The more complicated expression of the power spectrum coming out if

this change in the distribution function is taken into account has not been worked out in this paper, even if its behavior is qualitatively well understood and is in agreement with the experimental results of a "whitening" of the spectrum and a lowering of its intensity.

The temperature behavior of the total noise power intensity can be obtained by integrating Eq. (8) with respect to  $\omega$  from  $-\infty$  to  $\infty$ :

$$\begin{aligned} \frac{\langle \Delta G^2 \rangle}{\langle G \rangle^2} &= \int_{-\infty}^{\infty} \psi_F(\omega) d\omega \\ &= \frac{1}{48} \frac{e^2 \varphi_B^{-1}(T) kT}{\epsilon_0 \epsilon_r^* l} \\ &\quad \times \left( \frac{4\pi}{h} (2m)^{1/2} d - \varphi_B^{-1/2}(T) \right)^2 \frac{D^2 L}{L^{1/3}}. \end{aligned} \quad (9)$$

A plot of this quantity versus temperature is given in Fig. 6. Again, the drop experimentally observed at temperatures higher than 400 °K is due to the same reasons pointed out above and not taken into account by Eq. (9). Even the increase of the noise intensity at temperatures below 250 °K is not accounted for by Eq. (9). This effect is taking place because  $D$  is actually not independent of temperature, but should increase when temperature decreases. This apparently strange effect is due to the strongly different behavior of the conductivity versus temperature of metal islands separated by gaps having different widths: when the temperature decreases the conductivity between islands separated by larger gaps decreases much more rapidly (see Fig. 12). This fact increases the value of  $D$ , and thus also the value of the noise intensity. Actually, a more refined theory should take into account the real structure of the film by treating the gap widths as random variables, and defining  $D$  and  $l$  as suitable averages of quantities related to the potential drops of the applied voltage.

Finally, for what concerns the effects of gas diffusion and ion migration on the films conductance and noise, a quantitative description of the experimental results by the proposed theory has not been attempted yet. It may be noted, however, that the presence of impurity ions at the surface of the insulator can strongly change the energy and the density of the surface states, producing important shifts in the tunneling barrier height.

## V. CONCLUSIONS

In the preceding paper, a model which associates with a direct tunneling of the electrons a potential barrier modulation created by the surface states ionization is presented. The theoretical results obtained from this model, compared with the ex-

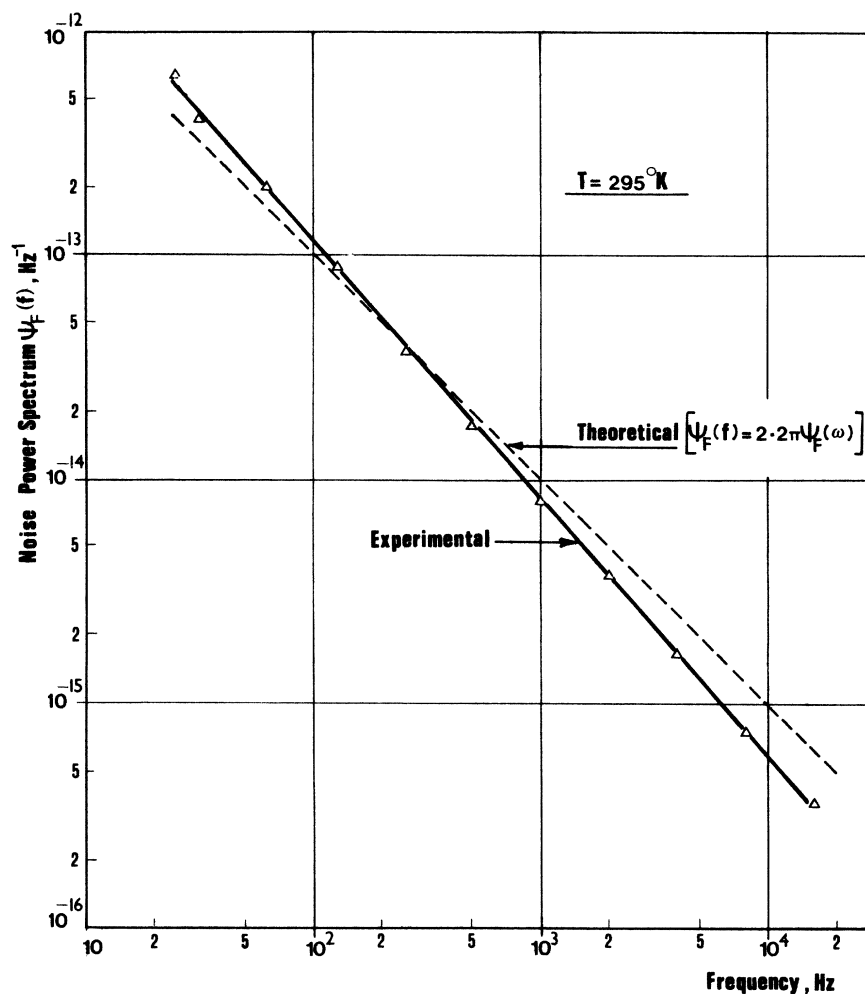


FIG. 13. Power spectra of the relative conductance noise  $\psi_r(f)$  at room temperature vs frequency. The points are experimental and refer to Au film evaporated onto sapphire substrate. Broken line is theoretical and is computed from Eq. (8) with  $\ln(\tau'_M/\tau'_m) = 16$ . The values of the other parameters are the same as in the caption of Fig. 11.

perimental data here reported, lead to the following conclusions:

(a) The electrical conductance behavior versus temperature predicted by the present theory finds an experimental confirmation over a very large range of temperatures, provided that the contribution of the thermionic current given by Eq. (6) is neglected. This fact is explained by observing that the mean free path of the electrons within the substrate and near its surface is probably smaller than the gap width between metal islands.

(b) When the electrical resistance of the film is changed by varying the average gap width between metal islands, the temperature coefficient of the resistance changes according to the provisions of the theory.

(c) For what concerns electrical noise, the theory gives the correct order of magnitude of the noise power spectrum, as against the small intensity of electrical noise found by the previous theory. The correct shape of the power spectrum

versus frequency is also obtained. Regarding the total noise dependence of the temperature in a fixed-frequency band, the theoretical model must be improved. The main difficulties in applying this model arise from the evaluation not only of the quantities related to a single gap, but also of those associated with the overall film structure. The hypothesis that the gaps are equal is quite crude. For this reason it may be expected that some theoretical results, like the absolute value of the total noise intensity, which are strongly influenced by the film structure, are not in good agreement with the experiments (Fig. 6). Actually, with high temperatures the distribution function for the ionization time is no longer  $1/\tau$ , since the electron transfer from the donor states to the metal may take place also through the electron excitation from the conduction band. With small temperatures, owing to a great variation of the electrical conduction, the parameters like  $D$  and  $l$  are no longer constant. An improved theory in this

direction must consider the gaps distribution and must take into account the relative stochastic variables. These considerations should be the subject of a theory that supplies a better picture of the film structure.

#### ACKNOWLEDGMENT

The authors wish to acknowledge Professor G. Montalenti for stimulating discussions and for providing the research facilities to carry out this study.

#### APPENDIX

In the following it will be shown that in a conduction mechanism where barrier-modulation effects are absent (simple tunneling, trap-assisted tunneling, thermionic effect), the current noise related to the conductivity fluctuation is many orders of magnitude smaller than the observed one.

Let us first calculate the conductance fluctuation spectrum for a pair of metal islands in the limit  $\omega \rightarrow 0$ . This will be an upper limit for the noise power density. In all the three cases considered above, the conductance between the two islands can be written in the form

$$G = \alpha S J_0, \quad (\text{A1})$$

where  $J_0$  is the tunneling (or thermionic) current density crossing the gap between the islands in both opposite directions when zero potential difference is applied to the gap in thermal equilibrium,  $S$  is the gap cross section, and  $\alpha$  is a proportionality factor which is actually very little dependent on the gap width and on the potential barrier height.

The physical meaning of  $\alpha$  is that it represents the inverse of the potential difference which should be applied to the islands pair to create a drift current density equal to  $J_0$ . Within an order of magnitude the value of  $\alpha$  can thus be taken as the inverse of the potential barrier height, and turns out in practical cases to be of the order of  $10 \text{ V}^{-1}$ . For instance, in the case of simple tunneling,<sup>21</sup> with the symbols used in the text,

$$\alpha = e[(d/\hbar)(2m)^{1/2}\varphi_B^{-1/2} - \varphi_B^{-1}]. \quad (\text{A2})$$

For barrier heights between 0.1 and 1 eV and  $d = 16 \text{ \AA}$  the value of  $\alpha$  ranges between 16 and  $7 \text{ V}^{-1}$ .

According to Eq. (A1), the fluctuation spectrum  $\phi_G(\omega)$  of  $G$  is simply proportional to the fluctuation spectrum  $\phi_I(\omega)$  of the current  $SJ_0$ :

$$\phi_G(\omega) = \alpha^2 \phi_I(\omega). \quad (\text{A3})$$

Taking into account that electron emission from metal islands is a Poisson process, the power spectrum  $\phi_I(\omega)$  in the limit  $\omega \rightarrow 0$  simply becomes

$$\phi_I(0) = eS J_0, \quad (\text{A4})$$

which corresponds to Schottky relation for the saturated diode. The relative conductance fluctuation spectrum for an island pair in the limit  $\omega \rightarrow 0$  thus yields

$$\psi(0) = \frac{\phi(0)}{G^2} = \frac{e\alpha}{G} \approx 10 \frac{e}{G}. \quad (\text{A5})$$

The last quantity in Eq. (A5) contains only the electron charge  $e$  and the conductance  $G$ , which is equal to the surface conductance of the film  $G_s$ , and it is an easily measurable quantity.

Finally, for the whole film, according to Eq. (35-I):

$$\psi_F(0) = \psi(0) \frac{D^2 L}{L'^3} = 10 \frac{e}{G} \frac{D^2 L}{L'^3}. \quad (\text{A6})$$

For the gold films used in experiments reported in this paper  $G_s \approx 2 \times 10^{-5} \Omega^{-1} \square$ ,  $D^2 L/L'^3 \approx 10^{-8}$ . From Eq. (A6) the value  $\psi_F(0) \approx 10^{-21}$  is obtained. This value is at least 12 orders of magnitude lower than the observed one, as seen from the data reported in Fig. 8.

It should be noted that the only quantity which is not directly measurable in Eq. (A6) is  $D$ . However, the factor  $D^2 L/L'^3$ , when  $L \approx L'$ , represents the inverse of the number of metal islands in the whole film, so that the value of this quantity can be estimated within one or two orders of magnitude by direct observation of the film structure.

\*Permanent address: Istituto di Fisica Generale, Università di Torino, Italy.

†Permanent address: Istituto di Fisica Sperimentale, Politecnico di Torino, Italy.

<sup>1</sup>R. C. Neugebauer and M. Webb, *J. Appl. Phys.* **33**, 74 (1962).

<sup>2</sup>J. G. Skofronick and W. B. Phillips, *Appl. Phys. Lett.* **7**, 249 (1965).

<sup>3</sup>L. A. Weitzenkamp and N. M. Bashara, *Trans. Metall. Soc. AIME* **236**, 351 (1966).

<sup>4</sup>D. S. Herman and T. N. Rhodin, *J. Appl. Phys.* **37**,

1594 (1966).

<sup>5</sup>K. Van Steensel, *Philips Res. Rep.* **22**, 246 (1967).

<sup>6</sup>R. M. Hill, *Proc. R. Soc. London A* **309**, 397 (1969).

<sup>7</sup>G. Dittmer, *Thin Solid Films* **9**, 317 (1972).

<sup>8</sup>L. L. Kazmerski and D. M. Racine, *J. Appl. Phys.* **46**, 791 (1975).

<sup>9</sup>B. Abeles, Ping Sheng, D. M. Coutts, and Y. Arie, *Adv. Phys.* **24**, 407 (1975).

<sup>10</sup>L. L. Kazmerski, D. M. Racine, and M. S. Ayyagari, *J. Appl. Phys.* **46**, 2658 (1975).

<sup>11</sup>M. Celasco, A. Masoero, P. Mazzetti, and A. Stepan-

- escu, Phys. Rev. B 17, 2553 (1978) (preceding paper); equations referring to paper I will be indicated in the following by the equation number followed by I.
- <sup>12</sup>A. Bobbio, A. Masoero, P. Mazzetti, and A. Stepanescu, Thin Solid Films 36, 33 (1976).
- <sup>13</sup>P. Mazzetti and A. Stepanescu, Thin Solid Films 13, 67 (1972).
- <sup>14</sup>M. Celasco and F. Fiorillo, Appl. Phys. Lett. 26, 213 (1975).
- <sup>15</sup>F. N. Hooge, Phys. Lett. 29A, 139 (1969).
- <sup>16</sup>T. E. Hartman, J. Appl. Phys. 34, 943 (1963).
- <sup>17</sup>A. R. von Hippel, *Les dielectriques et leurs applications* (Dunod, Paris, 1961), p. 373.
- <sup>18</sup>Massachusetts Institute of Technology, Technical Report No. 119, "Tables of Dielectrical Materials" Vol. V, p. 70 (1957).
- <sup>19</sup>J. L. Williams and R. K. Burdett, J. Phys. C 2, 298 (1969).
- <sup>20</sup>J. L. Williams and I. L. Stone, J. Phys. C 5, 2105 (1972).
- <sup>21</sup>J. G. Simmons, J. Appl. Phys. 34, 1793 (1963).

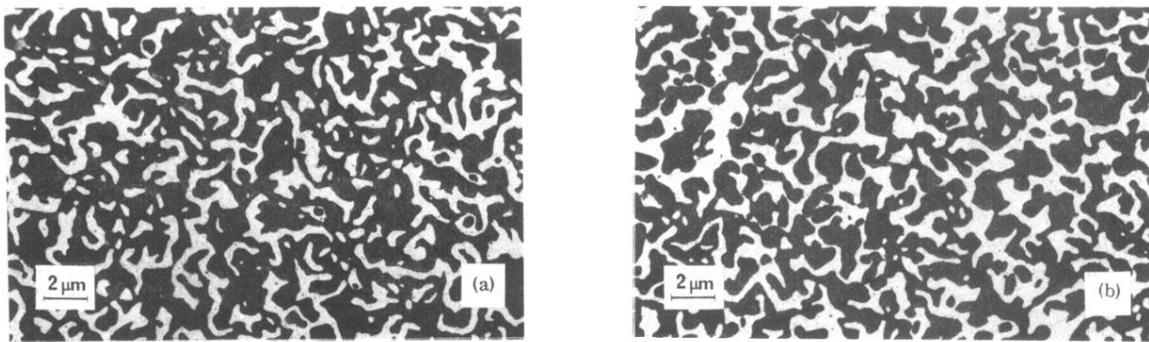


FIG. 1. Electron micrograph of discontinuous Au film structure on fused silica substrate after annealing at 500 °C in vacuum ( $10^{-9}$  mbar): (a) film with islands metallically connected and very low surface resistance ( $1.5 \Omega/\square$ ); (b) film with islands separated by very large gaps and practically infinite surface resistance.